TECHNICAL REPORT

Series No. 1, Issue No. 65a

THE COUPLED Q AND THE SHIFT IN RESONANT FREQUENCY OF SOME RESNATRON ANODE RESONATORS

by

Frederick B. Wood

Electronics Research Laboratory
Microwave Tube Group
Institute of Engineering Research
University of California
Berkeley, California

Contract Nos.:
W33(038)-ac-16649
W19(122)-ac-38

1 November 1953

FOREWORD

This report is a continuation of "Coupling between Waveguides and Cavity Resonators for Large Power Output", Series 1, Issue No. 65

The approximate theoretical analysis of the above report are applied to prototype resonators and specific resnatron anode resonators which have been built and tested on Contract Nos. W-19-122ac38 and W-33-038ac-16649 with the Air Material Command, USAF.

ABSTRACT

The basic procedure for obtaining the frequency shift and the coupled Q from an integral equation is reviewed. A method is outlined for using either theoretical or experimental results on prototype resonators in obtaining approximate values of Q_c and $\Delta f/f$ for other resonators.

The results for a TE_{101}-mode rectangular resonator and a TEM_{003}-mode coaxial resonator obtained in a previous report are discussed and are scaled to other frequencies. Calculations are made for a TM_{020}-mode cylindrical resonator at 9030 mc./s. by scaling experimental results on a TEM_{003}-mode resonator at 2820 mc./s. The scaling accounts for change of size with frequency and for change of stored energy with change of mode of oscillation. Close agreement between scaled values and experiment are obtained.

The anode resonators of the S-4 and S-6.01 resnatrons are unfolded and adjusted to simplified TM_{010}-mode coaxial and TM_{030}-mode radially stepped-cylindrical resonators respectively. Approximate calculations of Q_c and $\Delta f/f$ using the curves from the TEM_{003}-mode resonator plus the multiplying factors for the above simplified resonators give results within sixty percent of the experimental curves for the real S-4 and S-6.01 resonators. It is noted that this method uses the assumptions that the field distribution at the iris is similar for all resonators being compared, and that the electric radiation dipole moment is small compared with the magnetic dipole moment of the iris.

TABLE OF CONTENTS

LIST OF ILLUSTRATIONS

Figure

IX. INTRODUCTION

9.1 Summary of the Approximation Method

A theoretical analysis of the coupling between cavity resonators and waveguides has been developed.[1] Material in the previous report will be referred to directly by chapter, equation, and figure numbers, since this report is a continuation of the previous report. The basic principles of the analysis are as follows. A reference plane is selected in the waveguide at the iris for the definition of the voltage and current in the waveguide.

A resonator such as is shown in figure 9.1 is assumed to be excited by a generator at a distance down the waveguide. Then Poynting's theorem is applied to the electromagnetic waves at the reference plane in the waveguide. The magnetic field is expanded in terms of the following components: incident principal waveguide mode, reflected principal waveguide mode, reflected non-propagating waveguide modes, and resonator modes.

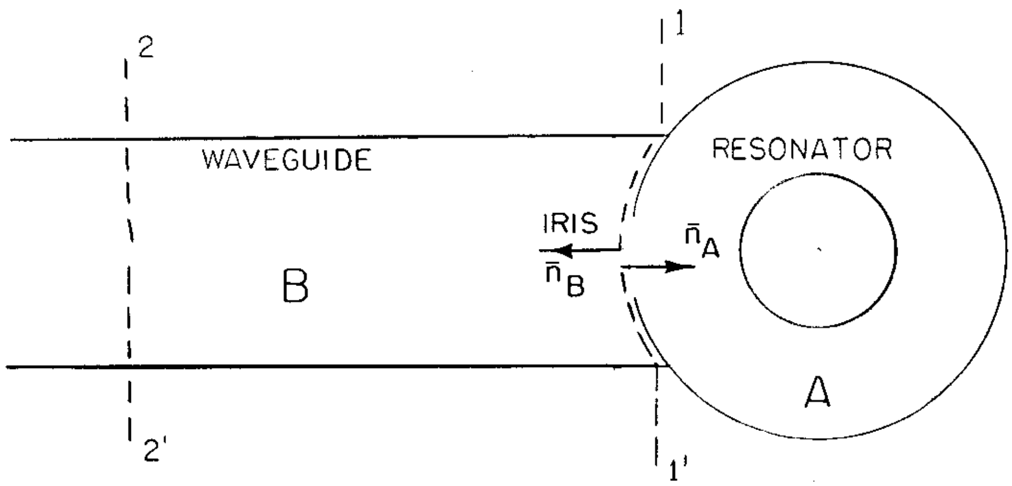

FIG. 9:1 IRIS COUPLING BETWEEN A WAVEGUIDE AND A CAVITY RESONATOR

1. Wood, F. B. Coupling between Waveguides and Cavity Resonators for Large Power Output. Univ. of Calif., Inst. of Engin. Research, Series Issue No. 65, May 1., 1953.

The current at the reference plane is defined so that the magnetic field is a sum of the vector modes

$$\bar{H}_i = I_i \; \bar{h}_i$$

where the amplitude coefficient, I_i is the defined as the current in the i-th mode and $\bar{h}_i$ is the orthonormal mode vector for the i-th mode.

Defining the voltage of the i-th mode as

$$V_i = \int \bar{h}_i \; (\bar{n} \times \bar{E}_i) \, dS \tag{9.1}$$

permits the equation for the power flow from Poynting's theorem to be manipulated into a stationary form for the input admittance of the resonator, referred to a second reference plane an integral number of half-wavelengths toward the generator from the first reference plane. The second reference plane is taken at a distance such that the higher modes in the waveguide have been attenuated to a negligible amplitude.

The resultant equation for the relative input admittance is

$$\frac{Y}{Y_0} = \frac{1}{Y_0} \left\{ Y'_B + N^2 \left[Y'_A + Y_{AO} \right] \right\} \tag{9.2}$$

which has the form of the following equivalent circuit.

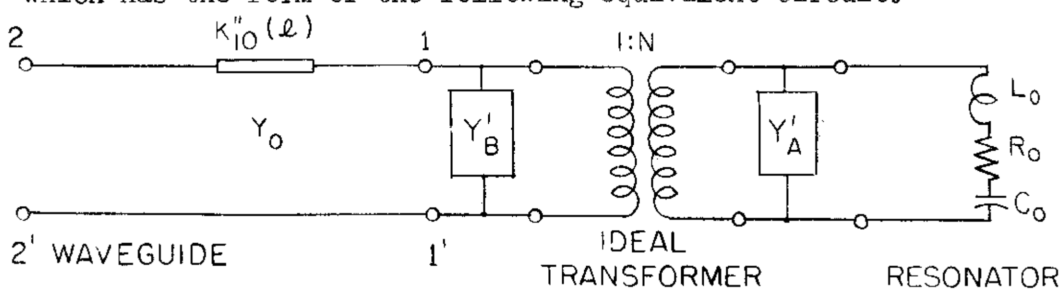

FIG. 9:2 EQUIVALENT CIRCUIT

Y_o is the characteristic admittance of the waveguide. Y_B is the admittance due to the reflected wave in the waveguide which is expressed as a sum of the higher non-propagating modes in the waveguides.

N is a transformer ratio which exists by reason of the different amplitude of the electric field excited in the iris by a unit amplitude normal principal mode in the waveguide and resonator. For the special case of the resonator having the same cross-section as the waveguide and having the same principal mode, the transformer ratio N would be unity.

The elements in equation (9.2) have stationary properities which can be demonstrated by putting the equation in the following form:

$$\frac{Y}{Y_o} = \frac{\omega\mu}{K_{10}''}\left\{ \begin{array}{l} + \dfrac{\int dS_r \int dS_s \left[\bar{n}_B \times \bar{E}(r)\right] \cdot \overleftrightarrow{\Gamma}_B^{(2)'}(r,s) \cdot \left[\bar{n}_B \times \bar{E}(s)\right]}{(V_A^o)^2} \\ + \left(\dfrac{V_A^o}{V_B^o}\right)^2 \left[\begin{array}{l} - \dfrac{\int dS_r \int dS_s \left[\bar{n}_A \times \bar{E}(r)\right] \cdot \overleftrightarrow{\Gamma}_A^{(2)'}(r,s) \cdot \left[\bar{n}_A \times \bar{E}(s)\right]}{(V_A^o)^2} \\ + \dfrac{j\omega}{\omega_o^2 - \omega^2 + j\dfrac{\omega\omega_o}{Q_o}} \end{array} \right] \end{array} \right\} \tag{9.3}$$

The unit normal vectors and the propagation constant can be identified from figures 9.1 and 9.2. $\bar{E}(r)$ is the assumed electric field in the iris, and $\overleftrightarrow{\Gamma}_A^{(2)}(r,s)$ and $\overleftrightarrow{\Gamma}_B^{(2)}(r,s)$ are the magnetic dyadic Green's functions for the resonator and the waveguide respectively.

The principal mode voltages V_A^o and V_B^o are defined for the resonator and waveguide respectively by equation (9.1). The resonant frequency ω_0 the Q_0 in equation (9.3) correspond to the lumped constant representation of the principal mode of the resonator shown in figure 9.2.

The susceptance in the waveguide, Y_B', and the susceptance in the resonator, Y_A' are stationary with respect to the first order variation of the electric field in the iris. The square of the transformer ratio, N^2 is stationary when the tangential components of the resonator and waveguide fields have the same form at the iris.

This means that if an approximation for the electric field in the iris is substituted into equation (9.3), the error in the circuit parameters will be proportional to the square of the fractional error introduced by the assumed field. Thus, if the assumed field has a small error, the resultant error will be smaller. The demonstration of these stationary properties is outlined in referencel, section 5.2. Details of the basic method can be found in Schwinger's lectures[2].

When the resonator and the waveguide have shapes for which the Green's function can be found, the substitution of a reasonable approximation for the iris field $\bar{E}(r)$ in equation (9.3) will give a good approximation to the input admittance. Then the resonant frequencies can be found by finding the zeros of the susceptance by

$$I_m \frac{Y}{Y_o} = 0 . \qquad (9.4)$$

The coupled Q can be calculated from a plot of the admittance near resonance. When the internal Q of the resonator is high as is usually the case in microwave resonators, the coupled Q can be reasonably approximated by using the following formula from lossles network theory:

$$Q_c = \frac{\omega}{2Y_o} \frac{\partial B}{\partial \omega} . \qquad (9.5)$$

Since most cavity resonators used in resnatron tubes have irregular cross-section, for which it is practically impossible to obtain Green's functions, a method of using simplified prototype resonators is developed. For simple resonators the resonant frequency and coupled Q can be calculated from equation (9.4) and (9.5) or they can be measured experimentally. The theoretical or experimental results can then be transferred into two sets of curves, the q-factor used in approximating the coupled Q and the v-factor used in estimating the shift in resonant frequency being defined as follows:

2. Saxon, David, S. Notes on Lectures by Julian Schwinger on Discontinuities in Waveguides. Feb. 1945. Reissued July 1953, Library of Congress, Photoduplication Service, Publication Board Project, PB 108834, (photostat and microfilm).

$$\frac{\Delta f}{f} = \frac{v}{4 N_r} \qquad (9.6a)$$

$$Q_C = Ng \cdot q \cdot N_r \qquad (9.6b)$$

$$N_r = \frac{U_E}{\mu |H|^2} \qquad \text{(RESONATOR)} \qquad (9.7)$$

$$Ng = \frac{8 S_a}{\omega \mu |H|^2} \qquad \text{(WAVEGUIDE)} \qquad (9.8)$$

$$S_a = \frac{1}{2} \int_{\substack{\text{CROSS SECTION OF} \\ \text{WAVEGUIDE}}} (\bar{n} \times \bar{E}_a) \cdot \bar{H}_a \, dS \qquad (9.9a)$$

$$U_E = \frac{1}{2} \int \epsilon |E|^2 dV \quad . \qquad (9.9b)$$

For small inductive irises the q-factor and v-factor reduce to the following where M is Bethe's magnetic dipole polarizability:[3]

$$q \rightarrow \left(\frac{\mu}{M}\right)^2 , \qquad (9.10) \qquad\qquad v \longrightarrow \left(\frac{M}{\mu}\right), \qquad (9.11)$$

---

3. Bethe, H.A. Lumped Constants for Small Irises. M.I.T., Rad. Lab. Report 194 (43-22), March 23, 1943. (Library of Congress, Publication Board Project, PB2839).

9.2 Application to a TE_{101}-mode Rectangular Resonator

In reference 1, the general analysis of Chapter V is applied to rectangular resonators in Chapter VI, and to coaxial resonators in Chapter VII. The theoretical results on the particular TE_{101}-mode rectangular resonator of figure 6.2 are plotted in Chapter VI. The shift in resonant frequency due to the coupling iris are plotted in figure 6.3. The curves of coupled Q are plotted in figure 6.4. These curves are then replotted as v-factor and q-factor curves in figures 6.5 and 6.6. These curves can then be used to approximate the $\Delta f/f$ and Q_c of other resonators having a similar field distribution at the iris by use of equations (9.5) through (9.8).

It should be noted that the v-factor and q-factor curves are limited to the same frequency range as the original resonator of figure 6.2, i.e. near 2965 mc./s. For other frequency ranges the curves must be scaled in proportion to the appropriate power of the wavelength. If the shape of the resonator and waveguide are geometrically the same as in the prototype resonator the $\Delta f/f$ and Q_c curves of figures 6.3 and 6.4 can be used directly without modification provided the same approximations as were used initially are still permissible.

From equations (6.30) and (6.31)

$$N_r = \frac{ab\lambda_g^3}{16\lambda^2} = \frac{abL}{8}\left(\frac{\lambda_g}{\lambda}\right)^2 = 39.8\times10^{-6}\ \text{METER}^3, \quad (9.12)$$

$$N_g = \frac{ab\lambda_g}{\pi} = 104\times10^{-6}\ \text{METER}^3.$$

For a frequency of 2965 mc./s.

$$q = \frac{Q_c}{N_g\cdot N_r} = 2.41\times10^8\, Q_c\ \text{METER}^{-6}, \quad (9.13a)$$

$$v = -\frac{4N_r\Delta f}{f} = -53.5\times10^{-9}\,\Delta f\ \text{METER}^3, \quad (9.13b)$$

where Δf is in mc./s.

If the resonator and waveguide are scaled from 2965 mc./s. to 9375 mc./s., a ratio which preserves (λ_g/a), the q-factor and v-factor become for $f'/f = 3.16$

$$q' = \left(\frac{f'}{f}\right)^6 q = 994\ q, \tag{9.14a}$$

$$v' = \left(\frac{f'}{f}\right)^{-3} q = \frac{v}{31.5} \tag{9.14b}$$

This scaling in frequency can be checked by examination of figure 6.2 of Ref. 1, and equations (6.27) and (6.29). From equations (6.29) and (6.30) it can be shown that if the ratios L/λ, b/a, and $\lambda g/\lambda$ are kept constant during the scaling of dimensions, that figures 6.3 and 6.4 give the $\Delta f/f$ and Q_c for any TE_{101}-mode rectangular resonator having the same geometrical ratios of its dimensions as that shown in figure 6.2.

To scale the results calculated for 2965 mc./s. to 9030 mc./s., the frequency of the resonator to be considered in section 9.4, it is necessary to make further corrections, because the above ratios are not preserved.

$$\frac{f'}{f} = 3.05\ , \qquad \frac{\lambda g}{\lambda} = 1.40\ , \qquad \frac{\lambda' g}{\lambda'} = 1.46$$

Using the approximation $Q'_c \simeq Q_c$, which is correct if the frequency is near 9375 mc./s. and the specified ratios are preserved, gives

$$\frac{q'}{q} = \left(\frac{f'}{f}\right)^6 \left\{\frac{\lambda g/\lambda}{\lambda' g/\lambda'}\right\}^4 = 698, \tag{9.15a}$$

$$\frac{v'}{v} = \left(\frac{f}{f'}\right)^3 \left\{\frac{\lambda' g/\lambda'}{\lambda g/\lambda}\right\}^3 = \frac{1}{25.3} \tag{9.15b}$$

For small irises, comparison of figures 3.4 and 6.5 and inspection of figure 7.2 show that the theoretical frequency shift is not reliable over the whole range of iris sizes. Therefore in some cases it is more useful to utilize an experimental curve of frequency shift as the basis for calculating the v-factor curves.

9.3 Application to a TEM_{003}-mode Coaxial Resonator

The close agreement of the experimental curves of q-factor for the TEM_{003}-mode coaxial resonator with the theoretical curves for the rectangular TE_{101}-mode resonator indicate that the curves of Q_c in figure 7.3 can be converted to q-factor curves for use in approximating the Q_c curves for other resonators. These curves for the TEM_{003}-mode resonator would be particularly valuable near the iris sizes having a width approximately equal to a half-wavelength. The theoretical analysis does not account for all the energy stored in the iris. In the region defined by radii r_2 and r_3 and width c in figure 7.1, only the principal waveguide mode is considered in the theoretical analysis.

The resonant frequencies of figure 7.2 are put in the form of the v-factor in figure 3.4. The curves are for a base frequency of 2820 mc./s. Examination of equations(3.10) and (9.6) show that for the TEM_{003}-mode, the v-factor is scaled in frequency as follows

$$\frac{v'}{v} = \left(\frac{f}{f'}\right)^3 = \left(\frac{2820}{9030}\right)^3 = \frac{1}{32.8} \qquad (9.16)$$

similarly

$$\frac{q'}{q} = \left(\frac{f'}{f}\right)^6 \left\{\frac{\lambda g/\lambda}{\lambda g'/\lambda}\right\}^{1} = 1100 \qquad (9.17)$$

9.4 Application to a TM_{020}-mode Cylindrical Resonator

In a previous report[4] experimental data is reported on the coupling of a TE_{10}-mode waveguide to a TM_{020}-mode cylindrical resonator by means of a rectangular iris. This particular study was done in connection with the investigation of a proposed resnatron anode resonator for a frequency of 2700 mc./s. However the experimental model was scaled in size to a nominal frequency of 9030 mc./s.

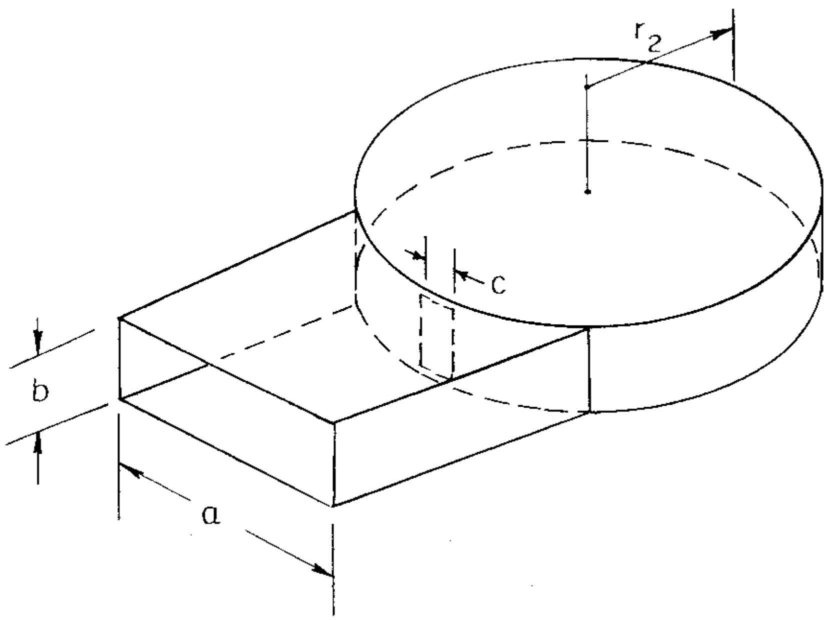

FIG. 9.3 IRIS COUPLING A TE_{10}-MODE WAVEGUIDE AND A TM_{020}-MODE CYLINDRICAL RESONATOR

4. Wood, F.B. Coupling of Power from a Resonant Circuit to Waveguide or Load at Microwave Frequencies. U. of C., Microwave Laboratory, Report 201, June 1, 1948. Figures 1B(1), 3, and 5.

For the cylindrical resonator shown in figure 9.3 at a nominal frequency of 9030 mc./s. the dimensions are, for λg = .048 meter

r_2 = 1.15" or .0292 meter,

a = 0.90" or .0229,

b = 0.40" or .0102.

From equations (9.7) and (9.8) the coefficients for the TE_{10}-mode in the waveguide are: $N_g = \frac{ab\lambda g}{\pi}$, (9.18a)

and for the TM_{020}-mode cylindrical resonator:

$$U_E = \pi bE_0^2 \frac{r}{2} J_1^2 (kr), \tag{9.18b}$$

$$k = \frac{x_{0,2}}{r_2} = \frac{5.52}{r_2}, \tag{9.18c}$$

$$H_\phi = j\sqrt{\frac{\epsilon}{\mu}}\, E_0 J_1 (kr), \tag{9.18d}$$

and
$$N_r = \frac{\pi b\, r_2^2}{2} . \tag{9.18e}$$

Substituting the numerical values into equations (9.18a) and (9.18e) gives

$$N_g = 3.56 \times 10^{-6} \text{ METER}^3, \tag{9.19a}$$

$$N_r = 13.6 \times 10^{-6} \text{ METER}^3. \tag{9.19b}$$

Then from equations (9.6a) and (9.6b) the following relations are obtained

$$V = \frac{-4N_r \Delta f}{f} = -6.03 \times 10^{-9} \Delta f \text{ METER}^3, \tag{9.20a}$$

with Δ f in mc./s.,

$$Q = \frac{Q_c}{N_r\, N_g} = 2.07 \times 10^{10}\, Q_c \text{ METER}^{-6}. \tag{9.20b}$$

APPROXIMATE CURVE OBTAINED BY TRANSFORMING EXPERIMENTAL RESULTS FOR $TEM_{0,0,3}$-MODE OF 2820 mc/s TO $TM_{0,2,0}$-MODE AT 9030 mc/s ——— *

EXPERIMENTAL CURVE FOR $TM_{0,2,0}$-MODE AT 9030 mc/s o— — —o— — —

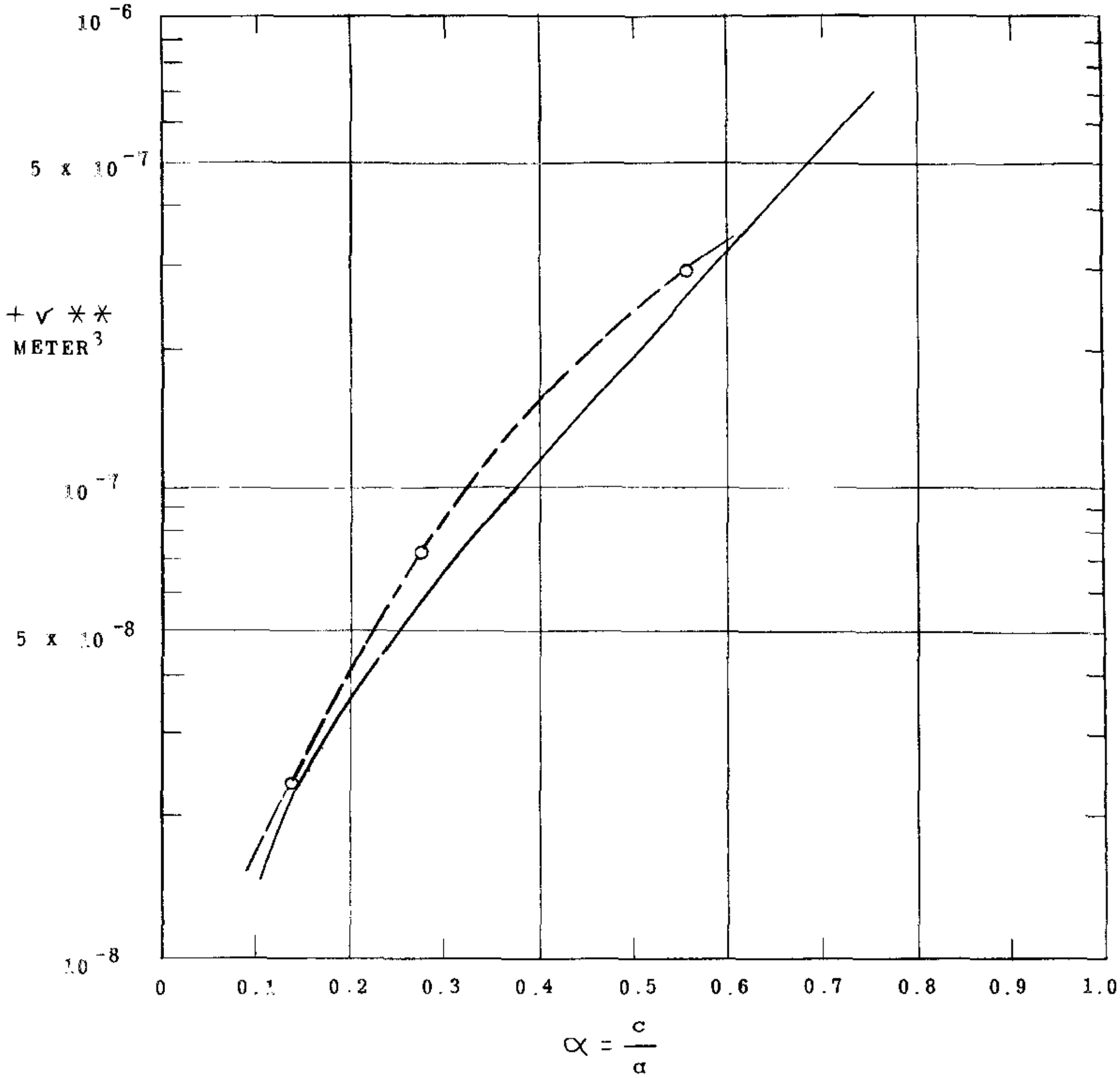

* v FROM EXP. RESULTS OF FIG. 3.4 DIVIDED BY 32.8
SEE EQUATION (9.16)

$$** \quad \Delta f = -\frac{v}{6.03 \times 10^{9}}$$

FIG. 9.4 FREQUENCY SHIFT VS. IRIS WIDTH FOR $TM_{0\,2\,0}$-MODE CYLINDRICAL RESONATOR

The experimental curve of Δf vs. iris width is converted to v vs. α by use of equation (9.20a) and is plotted in figure 9.4. An approximate curve of v vs. α is calculated from the experimental results of the TEM_{003}-mode coaxial resonator using frequency correction of equation (9.16). Three points of q are calculated from the experimental results and equation (9.20b) and are plotted in figure 9.5. An approximate curve is calculated from the experimental results for the TEM_{003}-mode coaxial resonator, using the frequency correction of equation (9.17) and is plotted in figure 9.5.

Examination of the experimental points for the TM_{020}-mode cylindrical resonator at 9030 mc./s. and the curves calculated for the same resonator by use of the experimental data on a TEM_{003}-mode coaxial resonator at 2820 mc./s. shows very close agreement in the region where the experimental accuracy is good. The point for $\alpha = .14$ in figure 9.5 which does not line up with the other points or with the calculated curve is for an iris width having a high standing wave ratio which could not be measured accurately with the equipment that was used. A similar situation exists for the smallest iris width shown in figure 10.3 for the S-4 resonator.

APPROXIMATE CURVE OBTAINED BY TRANSFORMING EXP. RESULTS
FOR TEM_{003}-MODE AT 2820 mc/s TO TM_{020}-MODE AT 9030 mc/s ——— **

EXPERIMENTAL POINTS FOR TM_{020}-MODE, 9030 mc/s o o

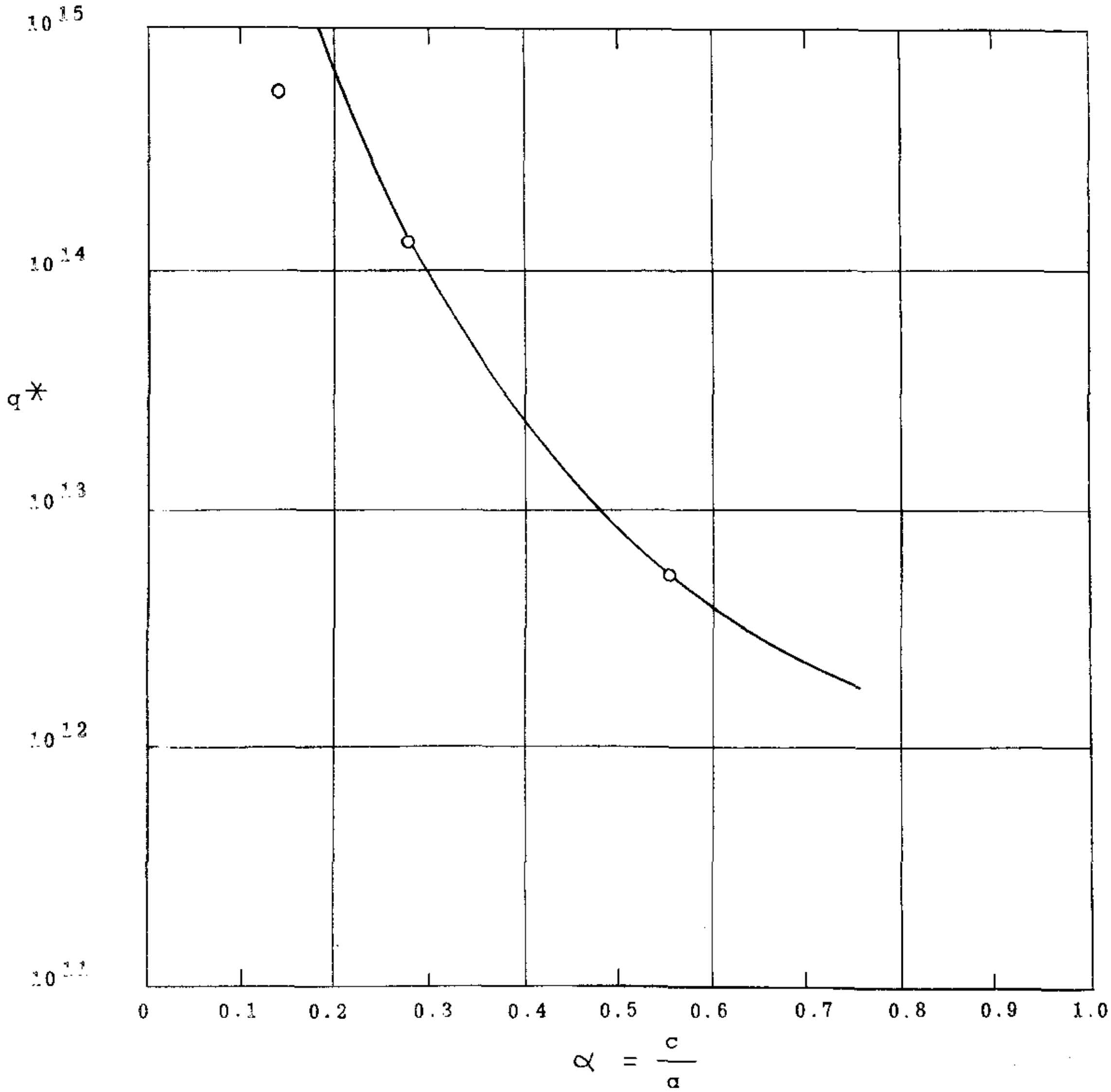

$$* \quad Q_c = \frac{q}{2.07 \times 10^{10}}$$

* * q^* FROM EXP. RESULTS OF FIG. 3.3 MULTIPLIED BY 1100.
SEE EQUATION (9.17)

FIG. 9.5 COUPLED Q VS IRIS WIDTH FOR $TM_{0.2.0}$-MODE CYLINDRICAL RESONATOR

X. APPLICATION TO PARTICULAR RESNATRON ANODE RESONATORS

10.1 S-4 Resnatron

The output coupling problem for the S-4 resnatron anode resonator has been experimentally analysed by Maltzer[5]. In this section approximate theoretical curves of $\Delta f/f$ and Q_c are obtained by use of the curves for prototype resonators in chapters III, VI, and VII. The theoretical curves are then compared with the experimental curves from Maltzer.

The actual resonator cross-section is shown in figure 10.1(a). The shape is too irregular to describe by simple mathematical functions. This simple radial line resonator has the same volume and the same resonant frequency as the actual resonator. The flat waveguide dimensions to replace the experimental waveguide are obtained by taking the average of the height b over the length corresponding to the waveguide coefficient N_g of equation (9.8).

The experimental results obtained by Maltzer for $\Delta f/f$ and Q_c are plotted in figures 10.2 and 10.3.

To calculate the frequency shift, the factor N_r must be determined. Using equations (9.7) and (9.9b), the following are obtained for the simplified TM_{010}-mode radial line (coaxial) resonator of figure 10.1(b). The stored energy is:

$$U_E = \frac{\pi h \epsilon}{2} r_2^2 Z_0'^2 (kr_2) \left[1 - \frac{r_1^2 Z_0'^2 (kr_2)}{r_2^2 Z_0'^2 (kr_3)} \right]$$

The magnetic field at r_2 is:

$$H = \epsilon B Z_0' (kr_2)$$

where
$$Z_0'(kr) = J_0'(kr) - \frac{J_0(kr2)}{N_0(kr_2)} N_0'(kr)$$

$$= \frac{J_0(kr_2)}{N_0(kr_2)} N_1(kr) - J_1(kr)$$

5. Maltzer, I. Cavity Waveguide Coupling by Large Iris, Institute of Engineering Research Report Series No. 1, Issue 43, Microwave Laboratory, University of California, Berkeley, June 1, 1951.

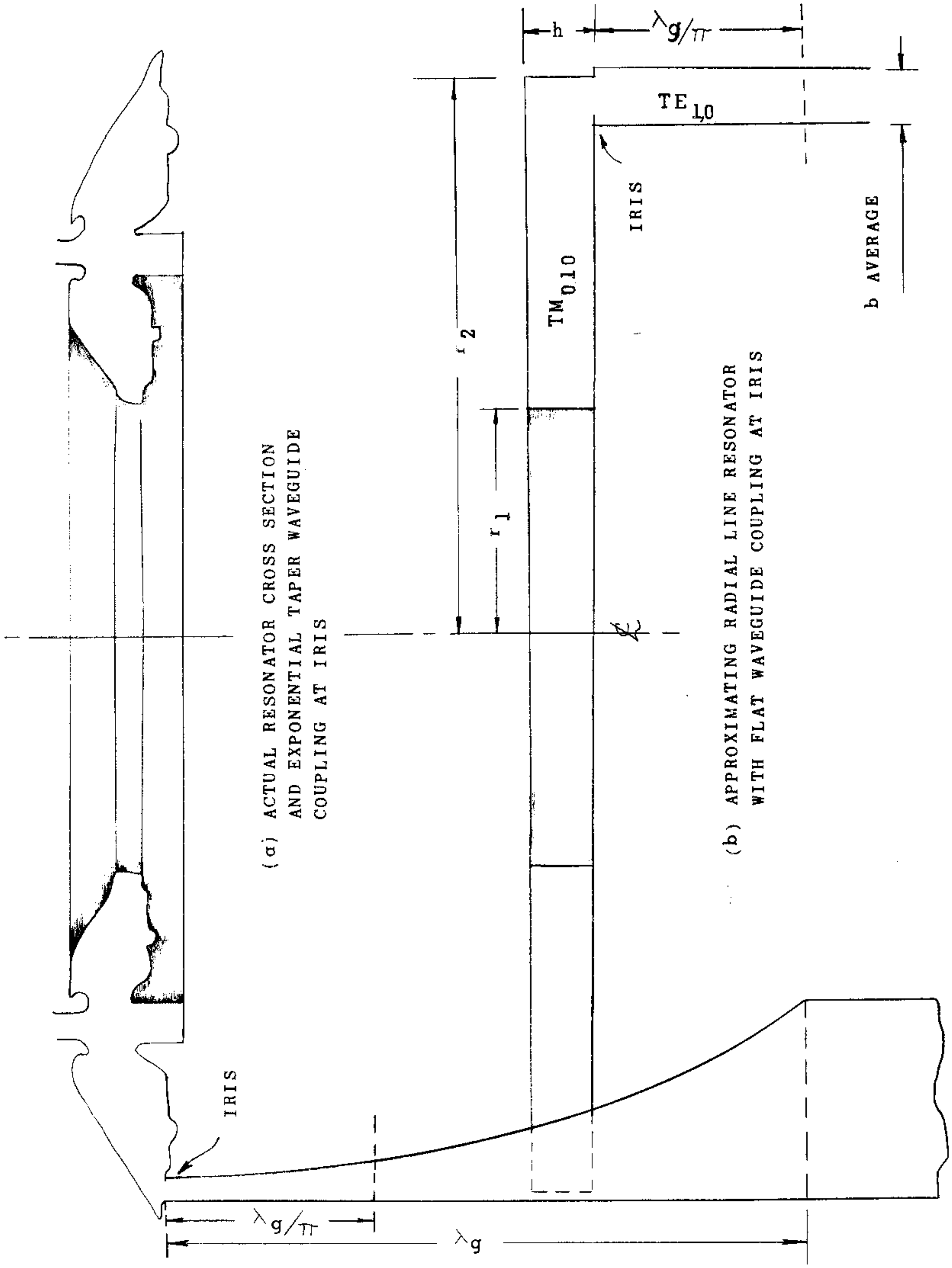

FIG. 10.1 S-4 RESNATRON ANODE RESONATOR

The normalization coefficents for the electromagnetic field are omitted here, because they would simply cancel out when inserted in equation (9.7). Since the center of the iris is not at r_2, an approximate value of the field at the iris is taken as

$$H_2' = 0.7\ H_2 . \qquad (10.1)$$

Putting these into equation (9.7) gives

$$N_r = \frac{\pi h r_2^2}{2} (0.7)^{-2} \left[1-0.48\right] \simeq \frac{\pi h r_2^2}{2} \qquad (10.2a)$$

Since the waveguide is in the TE_{10}-mode the N_g is the same as in equation (3.9)

$$N_g = \frac{a b \lambda_g}{\pi} . \qquad (10.2b)$$

Equation (10.2a) makes N_r have the order of magnitude of the volume of the resonator and equation (10.2b) sets N_g as the volume of a one-third wavelength piece of the coupling waveguide.

Since the waveguide is an exponential taper, the height b' in equation (10.3) is taken as the average height over the $\lambda g/\pi$ length of the waveguide starting from the iris. The numerical values are:

h = 0.430" or 0.0109 meter
r_2 = 3.64 " or 0.0925 meter
r_1 = 1.48 " or 0.0375 meter
a = 2.84 " or 0.0721 meter
λg = 0.1740 meter at f = 2728 mc./s.
b is a taper from .188" to .340" making b'=.260 or .0066 meter.
β = .188/1.340 = 0.14

$$N_r = 146.5\text{x}10^{-6}\ \text{meter}^3 \qquad (10.3a)$$

$$N_g = 25.9\text{x}10^{-6}\ \text{meter}^3 \qquad (10.3b)$$

Here the corrections to v and q for the operating frequency are neglected, because larger errors can easily be introduced in the simplification of resonator shape. The curves of $\frac{\Delta f}{f}$ in figure 10.2 are then obtained from equation (10.3a) and interpolating for β=.14

between the curves for the TEM_{003}-mode coaxial resonator of figure 3.4 and also interpolating from the curves for the TE_{101}-mode rectangular resonator of figure 6.5.

Calculating by equation (9.6a) for $v = 10^{-6}$ gives

$$\frac{\Delta f}{f} = -\frac{v}{4N_r} = -17.1 \times 10^{-4} \qquad (10.4)$$

The coupled Q is calculated from equation (9.6b) and figure 3.4 and 6.5, based on the experimental curve for the TEM_{003}-mode and the theoretical curve for the TE_{101}-mode respectively:

$$Q_c = N_g \cdot N_r \cdot q = 38 \times 10^{-10} q \;, \qquad (10.5)$$

$$\text{FOR } q = 10^{11},\; Q_c = 380.$$

The wall thickness correction T of figure 3.3 has been applied graphically to the curves of q from figure 6.5.

Summary for the Iris Width, α = 0.4

Approximation	Numerical Values	Ratio: Exp./Calc.
Rectangular TE_{101}-mode	$\Delta f/f$ = − 0.0061 Q_c = 290	1 / 1.53 2.8 / 1
Coaxial TEM_{003}-mode	$\Delta f/f$ = − 0.0037 Q_c = 520	1.08 / 1 1.56 / 1
Experimental S-4 Radial TM_{010} (Coaxial)	$\Delta f/f$ = − 0.004 Q_c = 810	

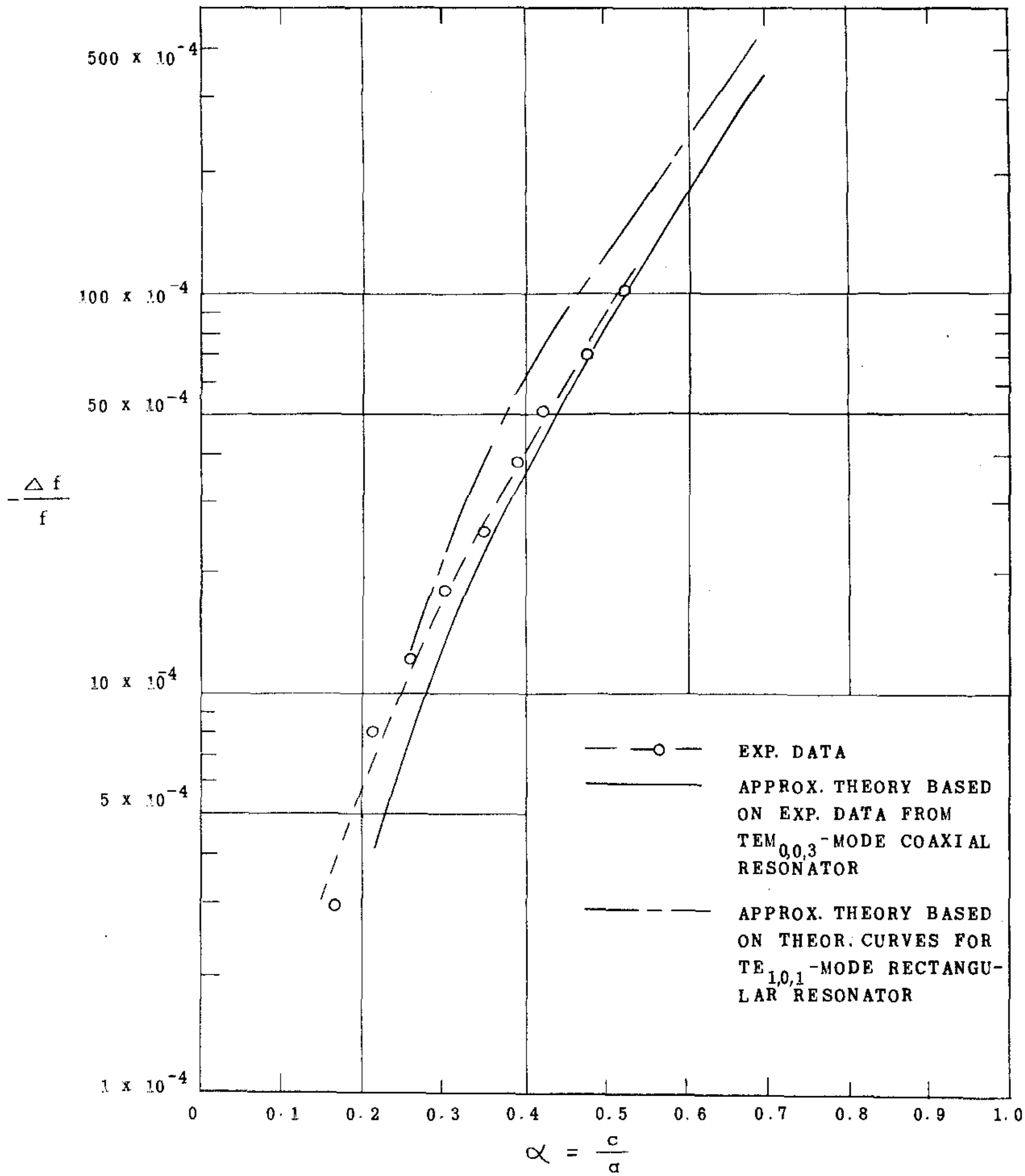

FIG. 10.2 FREQUENCY SHIFT VS IRIS WIDTH FOR S-4 ANODE RESONATOR

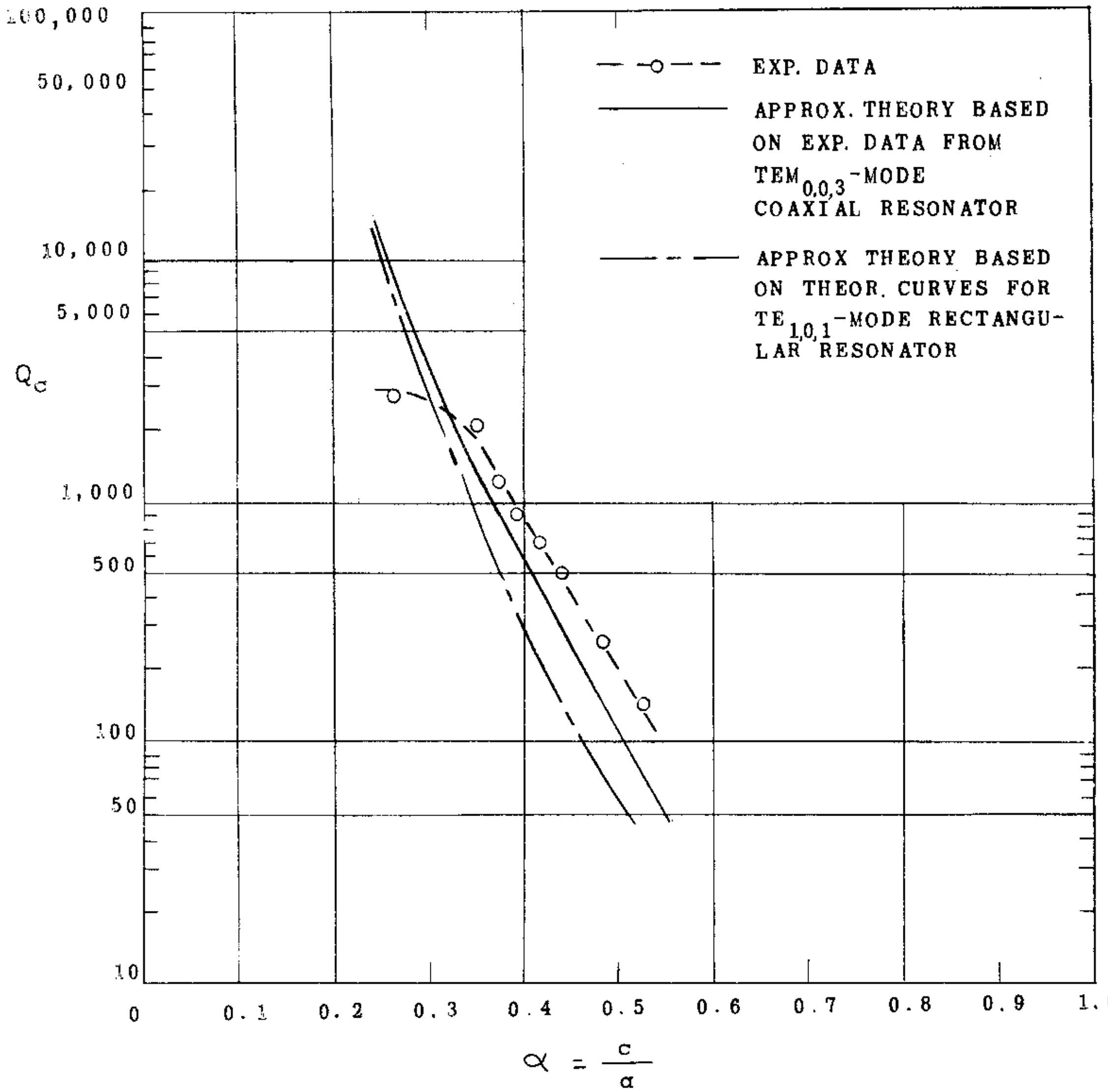

FIG. 10-3 COUPLED Q VS IRIS WIDTH FOR S-4 ANODE RESONATOR

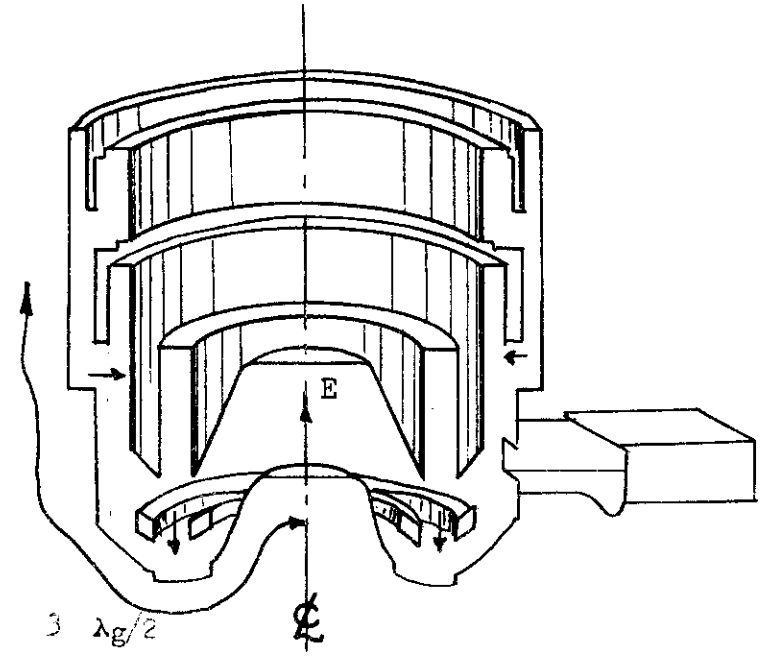

(a) Resonator Cross-Section

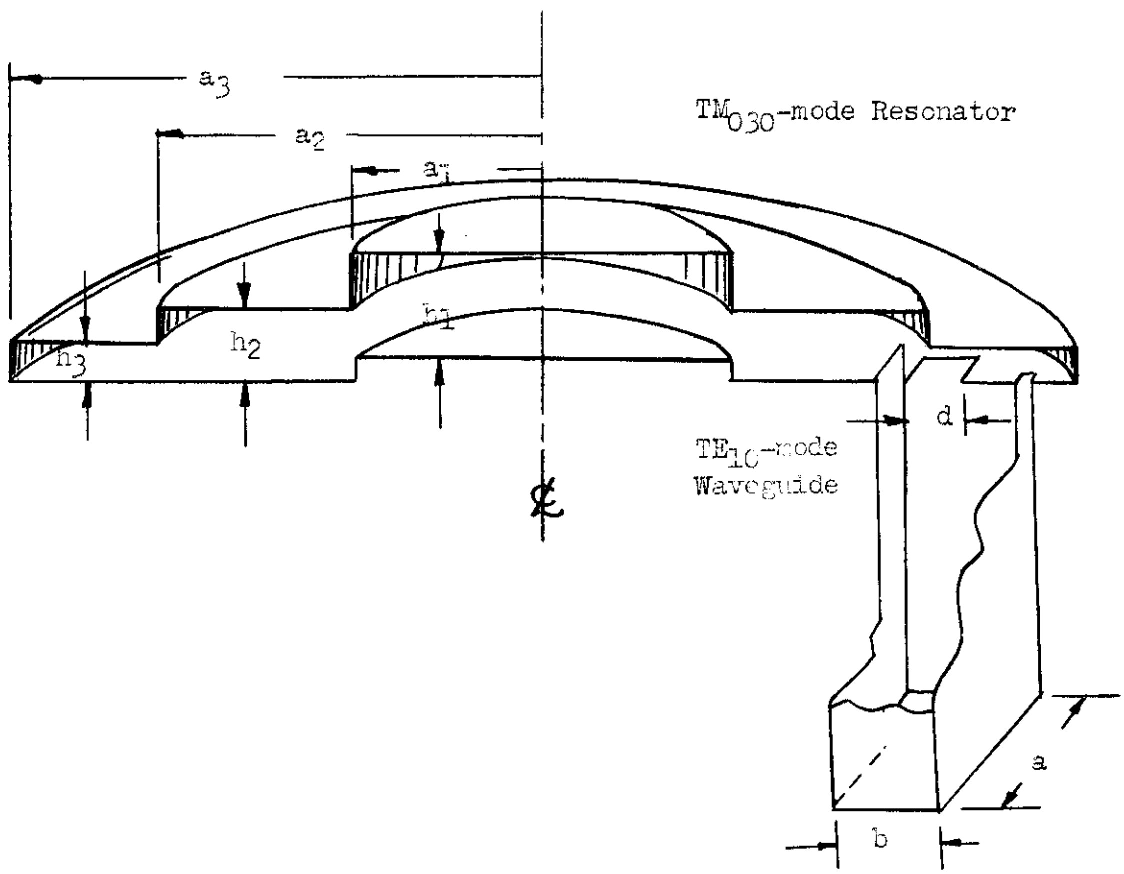

(b) Simplified Resonator and Waveguide

Fig. 10.4 Anode Resonator of S-6.01 Resnatron

10.2 S-6.01 Resnatron

A sketch of the cross-section of the anode resonator of the S-6.01 resnatron is shown in figure 10.4(a). It can be considered as a distorted form of a TM_{030}-mode cylindrical resonator or it can be considered as a folded radial line or as a composite of radial line and coaxial line sections. To obtain a simple approximate calculation of the coupled Q and frequency shift, the resonator is unfolded. Then by replacing the curved surfaces by equivalent flat rings and circular shells, the simplified resonator of figure 10.4(b) is obtained. In this approximation the volume of the different regions of the resonator are maintained constant through the transformation. No attempt is made to adjust the values of the electromagnetic field for the changes in contour and the omission of accelerating voltage rings.

By a graphical adjustment of the dimensions from the assembly drawing[6], the following dimensions are obtained for the simplified shape of figure 10.4(b) in M.K.S. units

a_1 = .056 meter h_1 = .028 meter
a_2 = .122 " h_2 = .024 "
a_3 = .175 " h_3 = .015 "

The waveguide dimensions are

a = 2.840" or .0721 meter

b = 0.750" or .0190 meter.

The iris dimensions are d = b, c = 1.965" or .0498 meter, making α = 0.692, and β = 0.554 (referred to standard waveguide).

The stored energy of the simplified resonator is U_E and the magnetic field at the center of iris is $H_{o\ell}$, so

$$U_E = \frac{\pi \epsilon E_0^2}{2} \left[h_3 a_3^2 \; J_1^2(ka_3) + (h_2 - h_3)\, a_2^2 \; J_1^2(ka_2) + (h_1 - h_2)\, a_1^2 \; J_1^2(ka_1) \right],$$

6. Microwave Laboratory Drawing No. 6S01A.

$Q_c = 285,$

$\Delta f/f = -.0061$

The calculated values are compared with the experimental values as follows:

Approximation	Calculated Values	Ratio: Exp./Calc.
Rectangular TE_{101}-mode	$\Delta f/f = -.0051$ $Q_c = 94$	1.2 /1 3.0 /1
Coaxial TEM_{003}-mode	$\Delta f/f = -.0040$ $Q_c = 180$	1.5 /1 1.6 /1

DISTRIBUTION LIST

No. of Copies	Organization
50	Commanding General Wright Air Development Center Ohio Attention: MCREES 23
35	Commanding Officer Air Force Cambridge Research Laboratories 230 Albany Street Cambridge, Massachusetts
2	Commanding Officer Rome Air Development Center Griffiss Air Force Base Rome, New York
1	Mr. John H. Hewitt Research Laboratory of Electronics Massachusetts Institute of Technology Cambridge, Massachusetts
2	Commanding Officer Office of Naval Research 1000 Geary Street San Francisco, California
10	Director, Institute of Engineering Research University of California Berkeley 4, California
25	File Microwave Tube Group University of California Berkeley 4, California